



Contents lists available at ScienceDirect

Vacuum

journal homepage: [www.elsevier.com/locate/vacuum](http://www.elsevier.com/locate/vacuum)

## Physical properties of TiO<sub>2</sub>-doped zinc oxide thin films: Influence of plasma treatment in H<sub>2</sub> and/or Ar gas ambient

Fang-Hsing Wang<sup>\*</sup>, Jen-Chi Chao, Han-Wen Liu, Feng-Jia Liu

Department of Electrical Engineering and Graduate Institute of Optoelectronic Engineering, National Chung Hsing University, Taichung 402, Taiwan, ROC

### ARTICLE INFO

#### Article history:

Received 30 June 2016

Received in revised form

31 October 2016

Accepted 5 November 2016

Available online xxx

#### Keywords:

Transparent conducting film

TiO<sub>2</sub>-doped zinc oxide

Magnetron sputtering

Plasma treatment

Hydrogen

### ABSTRACT

Transparent conducting TiO<sub>2</sub>-doped zinc oxide (ZnO:Ti, TZO) thin films were prepared by radio-frequency magnetron sputtering and followed by plasma treatments with different H<sub>2</sub>/(H<sub>2</sub> + Ar) flow ratio (R<sub>H2</sub>). The electrical, structural, and optical properties of the TZO thin films were investigated. Experimental results showed that resistivities of all the TZO thin films decreased after plasma treatment regardless of ambient gas, and the lowest resistivity was  $1.13 \times 10^{-3} \Omega\text{-cm}$  (or 62% reduction) for R<sub>H2</sub> = 50%. All the TZO thin films exhibited a (002) preferred orientation along the c-axis, indicating a typical wurtzite structure. Surface roughness of the TZO films slightly increased from 1.58 nm to 1.63–2.75 nm (RMS value) after plasma treatments. Average optical transmittance of the TZO films (containing glass substrates) in the visible region (400–700 nm) did not considerably change after plasma treatments and ranged from 82.7% to 84.3%. The largest figure of merit (FOM),  $5.02 \times 10^{-3} \Omega^{-1}$ , was achieved for the plasma-treated film with R<sub>H2</sub> = 50%, and it increased by 237% as compared with that of the as-deposited film. These results indicate that the H<sub>2</sub> + Ar (1:1) plasma treatment is more effective than pure H<sub>2</sub> or Ar plasma treatment in improving opto-electronic properties of transparent conducting TZO thin films.

© 2016 Elsevier Ltd. All rights reserved.

### 1. Introduction

Transparent conductive oxide (TCO) films have been extensively used in optoelectronic devices. Indium tin oxide (ITO) films are the commonly used transparent conductive oxide at present [1–3]. However, ITO films are unstable in high temperature environment and indium is rare and toxic; alternative materials for ITO films, therefore, are continually studied.

Impurity-doped zinc oxide (ZnO) films are promising substitutes to replace ITO films as transparent conducting films due to non-toxicity, abundance in nature, and chemical/thermal stability. The trivalent cation-doped ZnO films such as ZnO:Al [4–7], ZnO:Ga [8,9], and ZnO:In [9,10] present superior electrical conductivity and transparency over the visible spectrum and have been widely studied in past few years. The quadrivalent cation may provide two free electrons to contribute the conductivity in ZnO thin films. Titanium (Ti) is a quadrivalent cation and has a radius of 0.068 nm which is close to that of Zn (0.074 nm). Therefore, it is satisfactory as

a donor in ZnO. The Ti content in the ZnO film is an important parameter because excess Ti may exist in interstitial site and act as the scattering center. Only a small amount of doped Ti<sup>4+</sup> could contribute more electrons and avoid acting as scattering centers. A few researchers have studied the properties of TZO films [11–16]. For example, Chung et al. [12,13] investigated effects of Ti content, deposition pressure, and substrate temperature on TZO films prepared by radio-frequency (RF) magnetron sputtering. Our previous study [16] investigated influence of in situ hydrogen doping and substrate temperatures on physical properties of TZO thin films and achieved a low resistivity of  $9.2 \times 10^{-4} \Omega\text{-cm}$  under the process conditions: the H<sub>2</sub>/(H<sub>2</sub>/Ar) flow ratio of 7.5% and the substrate temperature of 373 K. Although these earlier literature indicated that the appropriate amount of Ti and H in TZO thin films and the optimal deposition parameters could enhance the opto-electronic characteristics of TZO thin films, many research efforts for further improvement on characteristics of various TCO thin films have been proposed continuously.

A few previous studies [17–24] make use of post-deposition treatments such as annealing and plasma treatment to enhance characteristics of TCO thin films. Fang et al. [17] studied the effects of vacuum annealing on the properties of the ZnO:Al (AZO) films

<sup>\*</sup> Corresponding author. 145 Xingda Rd., South Dist., Taichung City 40227, Taiwan, ROC.

E-mail address: [fansen@dragon.nchu.edu.tw](mailto:fansen@dragon.nchu.edu.tw) (F.-H. Wang).

and indicated that the annealing process led to improvement of (002) orientation, increased carrier concentration and band-gap of the AZO films. Oh et al. [18] described that the hydrogen annealing resulted in decreased resistivity and blue shift of absorption edge in transmission spectra of AZO films. Ohashi et al. [23] reported the influence of pulsed argon–hydrogen plasma on opto-electronic properties of ZnO films and concluded that hydrogen was actually a cause of shallow donors and hence increased carrier concentration of the films. We previously reported the effects of H<sub>2</sub> plasma treatment on the physical properties of AZO and TZO films with different substrate temperatures [6,24]. Those results motivated us to further study the characteristics of plasma treated TZO under different plasma conditions.

In this study, TZO films were prepared on glass substrates by using reactive RF magnetron sputtering and followed by plasma treatments under various H<sub>2</sub>/Ar flow ratios. The plasma treatment was performed with a plasma-enhanced chemical vapour deposition (PECVD) system because it is convenient and practical for large-area applications such as flat-panel displays and thin-film solar cells. Effects of various plasma treatments on structural, electrical, and optical properties of TZO films were explored.

## 2. Experiments

Zinc oxide (99.999%) powder mixed with 1.5 mol% titanium oxide (99.999%) powder was mixed to form a TZO composition. After being dried and ground, these TZO powders were calcined at 1273 K and then ground again. Next, the powders were uniaxially pressed into a pellet of 5-mm thickness and 2-inch diameter using a steel die. After debinding, the TZO pellet was sintered at 1623 K for 3 h to form a ceramic target for sputtering. The TZO thin films were prepared on glass substrates (Corning 1737 glass) in an RF magnetron sputtering system. The TZO films with a thickness of about 330 nm were deposited at substrate temperature of 573 K with an RF power of 100 W. The base pressure was  $6.67 \times 10^{-4}$  Pa ( $6.67 \times 10^{-6}$  mbar). The working pressure was maintained at  $6.67 \times 10^{-1}$  Pa ( $6.67 \times 10^{-3}$  mbar) in Ar (99.995%) gas. The substrate holder spun at 40 revolutions per min. After deposition, the TZO films were treated by plasma under various H<sub>2</sub>/Ar flow ratios at 573 K for 60 min by using a parallel-plate PECVD system.

The film thickness was determined by a spectroscopic ellipsometer (Nano-view, SE MF-1000). The structure of the TZO film was examined by X-ray diffraction (XRD) (PANalytical) analysis with Cu-K $\alpha$  radiation ( $\lambda = 1.54056$  Å,  $\theta - 2\theta$  scan mode). The morphology of the TZO films was observed using a field emission scanning electron microscope (FE-SEM) (JEOL, JSM-6700) and an atomic force microscope (AFM) (Digital Instrument, NS4/D3100CL/Multimode). The resistivity, Hall mobility, and carrier concentration were measured using the Van der Pauw method (BIO-RAD, HL5500IU) at room temperature. The optical transmittance was measured by a UV/VIS/NIR spectrophotometer (Jasco V-570) in the 220–2500 nm wavelength range.

## 3. Results and discussion

The influence of RF power of the post-deposition plasma treatment on resistivity of TZO thin films was investigated and shown in Fig. 1. The plasma treatment time is 60 min. Results show the film resistivity decreased with increasing RF power up to 80 W, then increased for a further increase in RF power. It is considered that high RF power could increase the ion energy in plasma, which enhances hydrogen doping, surface cleaning, and annealing effect. However, a higher RF power than 80 W might result in high energetic ion bombardment leading to deteriorate the structure of the films. Thus, the following experiments were performed with a fixed

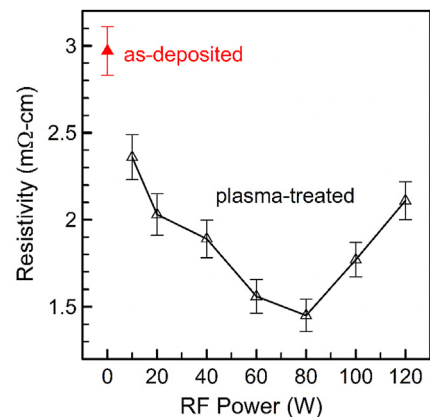


Fig. 1. Resistivity of TZO thin films as a function of RF power of the post-deposition plasma treatment.

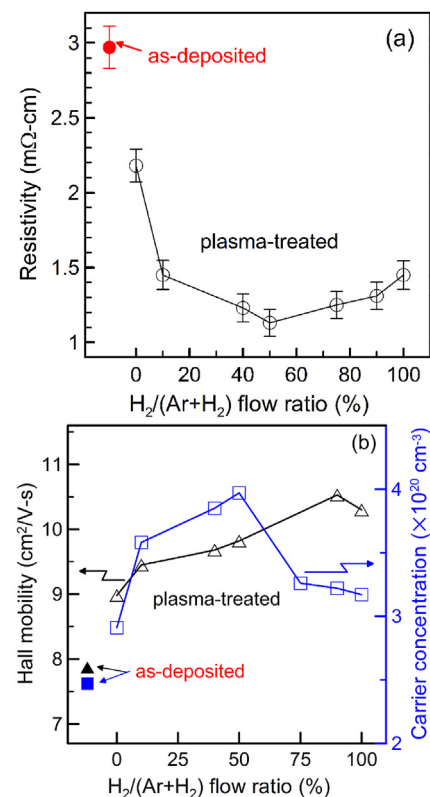


Fig. 2. Resistivity, Hall mobility, and carrier concentration for the as-deposited and various plasma treated TZO films.

RF power of 80 W during plasma treatments.

Fig. 2 shows the resistivity, Hall mobility, and carrier concentration of TZO thin films treated by plasma with various H<sub>2</sub>/(H<sub>2</sub>+Ar) flow ratio (R<sub>H2</sub>). The resistivity, Hall mobility, and carrier concentration of the as-deposited film were  $2.97 \times 10^{-3}$  Ω-cm,  $7.84$  cm<sup>2</sup>/V-s, and  $2.47 \times 10^{20}$  cm<sup>-3</sup>, respectively. After plasma treatment, the film resistivity remarkably decreased regardless of flow ratio compared to the as-deposited sample. The plasma treatment with R<sub>H2</sub> = 50% achieved the lowest resistivity of  $1.13 \times 10^{-3}$  Ω-cm, a reduction of 62% as compared to the as-deposited films. We previously reported that in situ hydrogen doping and pure hydrogen plasma treatment effectively improved the conductivity of TZO thin films [16,24]. For the 573 K-deposited TZO thin films, the former

reduce the resistivity by 30% (from 2.97 to 2.07 m $\Omega$ -cm) with 1% hydrogen in Ar ambient; while the later reduce the resistivity by 51% (from 2.97 to 1.45 m $\Omega$ -cm) with  $R_{H_2} = 100\%$  and a treatment time of 1 h at 573 K. In this work, we demonstrate that an appropriate  $H_2/(H_2+Ar)$  flow ratio (i.e.  $R_{H_2} = 50\%$ ) in plasma gas is more effective in improving the conductivity of TZO thin films than those earlier studies [16,24]. In the  $H_2+Ar$  plasma atmosphere, Ar ions may collide with H ions and film surface and thus increasing the hydrogen ionization efficiency and clean the film surface. These phenomena imply that the  $H_2+Ar$  plasma may produce more hydrogen, which may contribute to shallow donor formation, surface/defect passivation, and extraction of oxygen from the TZO films by H-atoms [30]. It is worth noting that the pure Ar plasma treatment ( $R_{H_2} = 0\%$ ) also causes a reduction of 27% in the resistivity of TZO films. This improvement may be attributed to hydrogen doing/passivation effect from a small amount of residual hydrogen and  $H_2O$  vapor in the PECVD chamber, and Ar cleaning effect through removing the chemisorbed oxygen on film surface and grain boundaries [19], as well as annealing effect during the 573 K plasma treatment. Cai et al. reported that the incorporated hydrogen in  $H_2$  plasma treated ZnO films not only passivated most of defects and present acceptors, but also introduced shallow donor states such as the  $V_O-H$  complex and the interstitial hydrogen  $H_i$  [25]. Besides, the incorporated hydrogen might remove negative charged oxygen species on the grain boundaries which formed depletion regions near the grain boundaries decreasing carrier concentration and Hall mobility [7,18,26]. The fact that the increments of the carrier concentrations of the  $H_2$ -containing plasma treated films are more than that of the pure Ar plasma-treated film supports these arguments, as Fig. 2(b) shows. The Hall mobilities of the  $H_2$ -containing plasma-treated films markedly increased in comparison with that of the pure Ar plasma-treated one. It may be attributed to desorption of oxygen species on film surface and grain boundaries, hydrogen passivation of defects, as well as the reaction of Ti replacing Zn through hydrogen incorporation, which decreases segregate Ti and related defects in grain boundaries [22,23]. The increased carrier concentration and Hall mobility both contributed to the decrease of the film resistivity and the optimal resistivity was obtained with the Ar/( $H_2 + Ar$ ) flow ratio of 50%.

Fig. 3 exhibits the  $\theta-2\theta$  XRD spectra of the TZO films prepared without and with various plasma treatments. All TZO films had only a (002) preferred orientation, regardless of plasma treatment. It is attributed to ZnO thin films having lowest surface energy at (002) crystal orientation and thus the continuous growing of the films along this orientation. Moreover, film crystallinity slightly varied with different plasma treatments. The  $2\theta$  angle of (002) peak shifted from 34.30° slightly to the higher angle of 34.37° for the Ar and  $H_2 + Ar$  plasma-treated samples, while it was almost the same

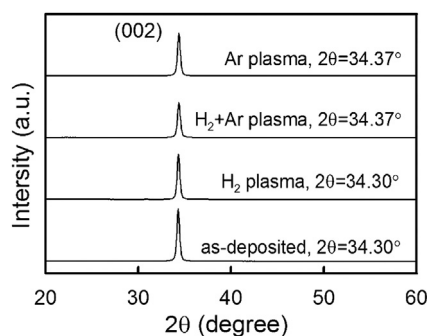


Fig. 3. X-ray diffraction spectra of the TZO films without and with various plasma treatments.

for the  $H_2$  plasma-treated one. Oh et al. reported that the position of the ZnO (002) peaks shifted toward higher diffraction angles from 34.32° to 34.36° as hydrogen annealing time increased, implying relaxation of the residual strain introduced in the films during the deposition process [18]. On the other hand, Liu et al. reported that a smaller diffraction angle ( $2\theta$ ) was found for Al-doped ZnO films sputtered in Ar +  $H_2$  ambient due to that hydrogen atoms were situated in the Zn–O bond centers [27]. The plasma treatment may cause thermal annealing effect and hydrogen incorporating into films. The former results in residual strain relaxation and increases the diffraction angle, while the latter decreases it [7,18,27,28]. Results reveals that effect of thermal annealing is larger than that of hydrogen incorporating into films for the Ar and  $H_2 + Ar$  plasma-treated samples, while these two effects balance for the  $H_2$  plasma-treated case.

Fig. 4 shows the full-width at half-maximum (FWHM) and the grain size of the TZO films without and with various plasma treatments. The grain size is estimated using Scherrer's formula [29],

$$D = \frac{0.94\lambda}{\beta \cos \theta} \quad (1)$$

where  $\lambda = 0.154056$  nm,  $D$  is grain size and  $\beta$  is FWHM. The Ar plasma-treated film exhibited the smaller FWHM value, indicating the larger grain size than the others. It may be attributed to the thermal annealing effect during Ar plasma treatment. The grain sizes for the  $H_2$  and Ar +  $H_2$  plasma-treated films slightly decreased after treatment. However, the differences of the grain sizes between different plasma treatments were not obvious.

Fig. 5(a–d) display the FE-SEM micrographs of the TZO films before and after various plasma treatments. The surface morphology of the as-deposited film showed continuous and dense surface grains. This result is similar to the observation of Chung et al. [12]. From Fig. 5(b–c), it could be seen that surface grains were etched and a lot of small holes appeared. This phenomenon may result from etching effect of hydrogen radicals. Baik et al. had investigated effects of hydrogen plasma treatment performed by photochemical vapor deposition on ZnO films and concluded that the film surface was etched by the hydrogen treatment process [22]. The surface roughness of the as-deposited and the various plasma-treated TZO films was also investigated by AFM, as Fig. 6(a–d) show. The scan area is 1  $\mu\text{m} \times 1 \mu\text{m}$  for all samples. The root-mean-square (RMS) roughness of the as-deposited film was 1.58 nm, while it increased to 2.75, 1.97, and 1.63 nm for the  $H_2$ , Ar +  $H_2$ , and Ar plasma-treated films, respectively. The data indicates that more hydrogen in the plasma ambient makes film surface rougher. It is believed that hydrogen radicals etch small

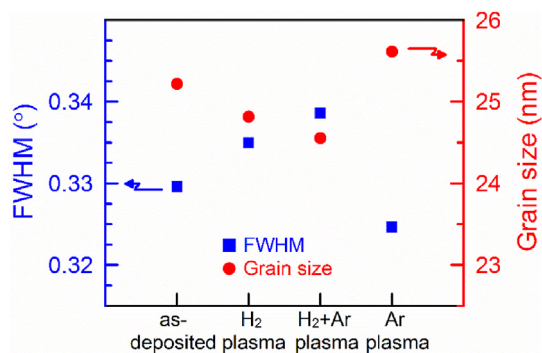


Fig. 4. Full-width at half-maximum and grain size of the TZO films without and with various plasma treatments.

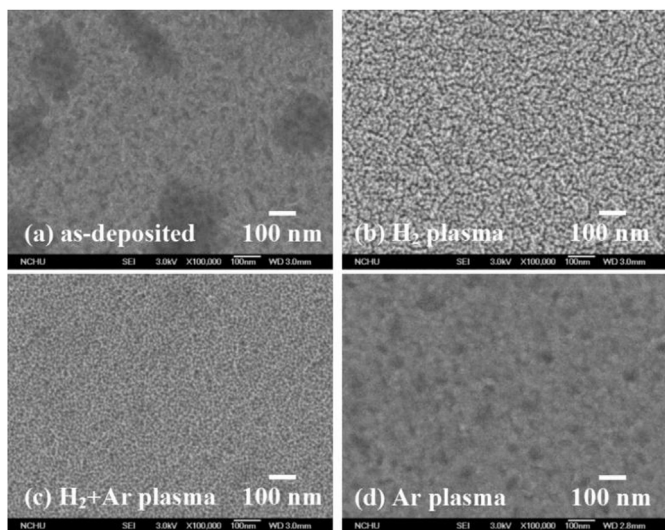


Fig. 5. FE-SEM micrographs of the TZO films: (a) as-deposited, (b) H<sub>2</sub> plasma treated, (c) H<sub>2</sub> + Ar plasma treated, and (d) Ar plasma treated.

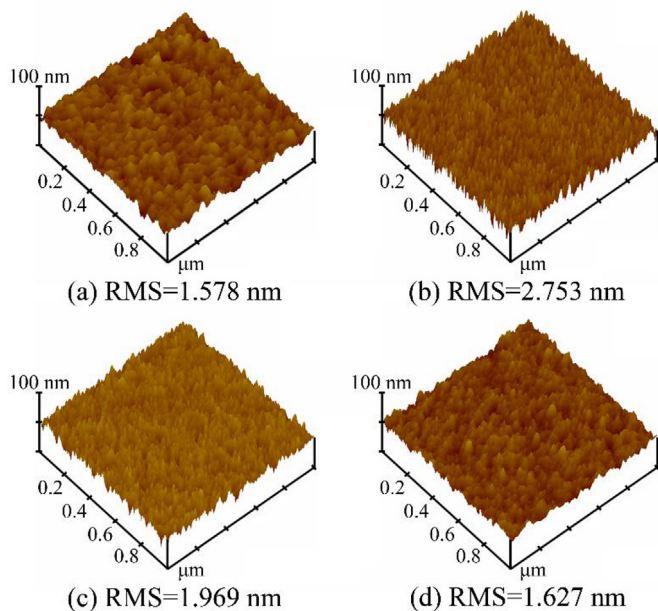


Fig. 6. AFM images of the TZO films over 1  $\mu\text{m} \times 1 \mu\text{m}$  area: (a) as-deposited, (b) H<sub>2</sub> plasma treated, (c) H<sub>2</sub> + Ar plasma treated, and (d) Ar plasma treated.

grains growing among large ones on the film surface [22]. This result is in accordance with the observations in Fig. 5.

Fig. 7 shows the optical transmittance spectra and the optical energy band-gap ( $E_g$ ) for the as-deposited and the various plasma-treated TZO films. The light illuminated from the glass side. From Fig. 7(a), after transmission through the substrate and TZO film, all the films had high average optical transmittances (>82%) in the visible wavelength region (400–700 nm) and strong absorption in the UV region. After plasma treatment, the average visible transmittance seemed no significant change for the different plasma treated samples. This behavior is similar to those observed in the work of Das et al. [30]. They also reported the transmission of the ZnO films prepared with Ar or Ar + H<sub>2</sub> remained unaltered after hydrogen plasma exposure [30]. However, it has been reported that

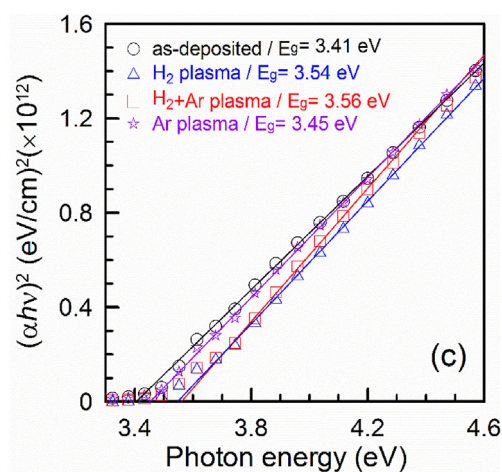
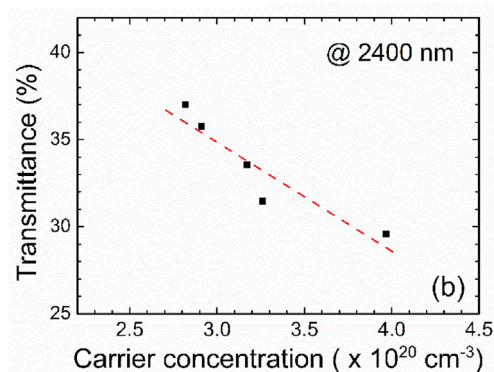
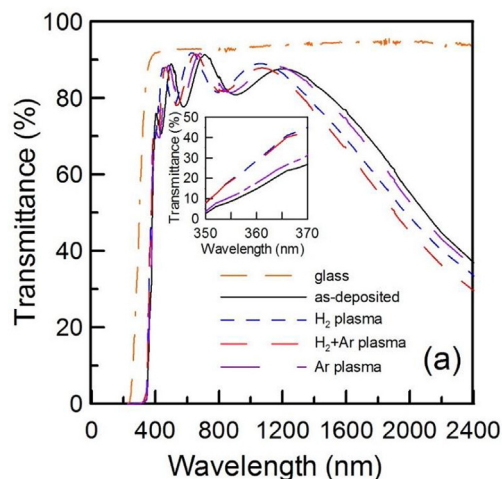


Fig. 7. (a) Optical transmittance spectra and (b) optical energy band-gap ( $E_g$ ) for the as-deposited and various plasma-treated TZO films.

the plasma-treated ITO and SnO<sub>2</sub> films showed only 60% transmittance in the visible range [31]. It is evident that the stability of the optical transmittance of the TZO film under plasma exposure is better than ITO and SnO<sub>2</sub> films. The high visible transmittance after plasma exposure demonstrated that the developed TZO films exhibited superior stability of optical properties for TCO applications. Furthermore, the inset figure exhibited that the absorption edges of the plasma-treated samples shifted to the short wavelength side in comparison with that of the as-deposited one. The blue shift of the absorption edge could be explained by broadening of optical band-gap, as discussed later. In near IR region, the optical transmittances decreased with the increasing wavelength and the

decrement was larger for the plasma-treated samples. From Fig. 7(b), it was observed that the transmittance at 2400 nm decreased with increasing carrier concentration for these TZO films. This result suggests that the decrease in NIR transmittance is due to free carrier absorption. This type of IR cut-off material was reported by Das et al. [30,32].

Fig. 7(b) shows the graph of  $(\alpha h\nu)^2$  vs. photon energy of the TZO films. The optical absorption coefficient,  $\alpha$ , is defined as [33].

$$I = I_0 e^{-\alpha t} \quad (2)$$

where  $I$  is the intensity of transmitted light,  $I_0$  is the intensity of incident light, and  $t$  is the film thickness. In the direct transition semiconductor,  $\alpha$  and the optical energy band-gap ( $E_g$ ) are related by [34].

$$\alpha h\nu = A(h\nu - E_g)^{1/2} \quad (3)$$

where  $h$  is Planck's constant,  $\nu$  is the frequency of the incident photon, and  $A$  is a constant. When  $(\alpha h\nu)^2$  is plotted against  $h\nu$ ,  $E_g$  can be estimated by extrapolating the linear portion against  $h\nu$ . The plot showed that the calculated  $E_g$  increased from 3.41 eV (as-deposited) to 3.54, 3.56, and 3.45 eV, respectively, for the H<sub>2</sub>, Ar + H<sub>2</sub>, and Ar plasma-treated films. The broadening of band-gaps agrees with the increases of the carrier concentrations, as Fig. 2(b) shows. This phenomenon consists with the Burstein–Moss effect [35], which indicates that the increase of the Fermi level in the conduction band of degenerate semiconductor leads to energy band-gap widening (blueshift effect). The energy band-gap widening ( $\Delta E_g$ ) is related to the carrier concentration ( $n_e$ ) through the following equation,

$$\Delta E_g = \frac{h^2}{8m^*} \left(\frac{3}{\pi}\right)^{2/3} n_e^{2/3} \quad (4)$$

where  $h$  is Planck's constant and  $m^*$  ( $m^* = 0.28 m$  [36]) is the electron effective mass in conduction band. Fig. 8 shows the blueshift (the difference of the band-gap) of the TZO films as compared to the stoichiometric ZnO film ( $E_g = 3.3$  eV) as a function of carrier concentration [35–37]. The blueshift of TZO films was approximately proportional to  $n_e^{2/3}$  and the experimental exponent in this study was 0.65, which was close to the theoretical value (0.667) in Eq. (4). This result shows that the optical band-gap of these TZO films follows the Burstein–Moss effect without the many-body perturbation effect [38].

Fig. 9 exhibits the figures of merit for the as-deposited and the various plasma-treated TZO films. The figure of merit, FOM ( $\rho = T^{10}/R_s$ , as defined by Haacke [39]), provides a way for

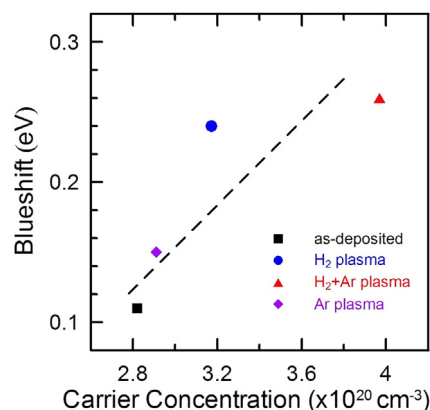


Fig. 8. Optical band-gap widening (blueshift) as a function of carrier concentration.

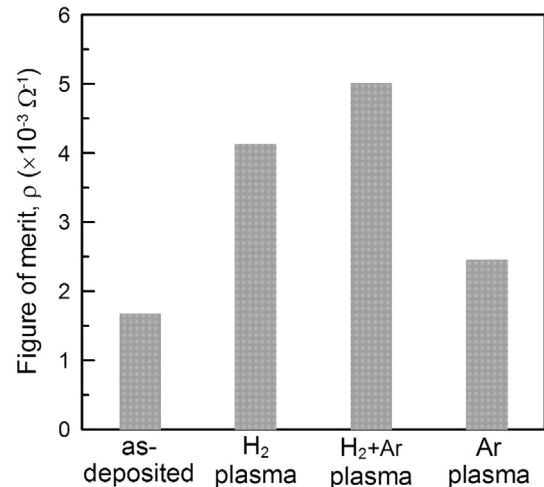


Fig. 9. Figures of merit for the as-deposited and various plasma-treated TZO films.

evaluating the opto-electronic properties of TCO films.  $T$  is the average optical transmittance in the visible wavelength region and  $R_s$  is the sheet resistance of films. The result showed that  $\rho$  increased from  $1.49 \times 10^{-3}$  (as-deposited) to  $4.38 \times 10^{-3}$ ,  $5.02 \times 10^{-3}$ , and  $2.26 \times 10^{-3} \Omega^{-1}$  for the H<sub>2</sub>, Ar + H<sub>2</sub>, and Ar plasma-treated films. This result indicates that the Ar + H<sub>2</sub> plasma-treatment is more effective than H<sub>2</sub> and Ar plasma treatment in improving opto-electronic properties of the TZO thin films.

#### 4. Conclusions

The structural, electrical, and optical properties of TZO thin films deposited by RF magnetron sputtering are dependent on the ambient gas of the post-deposition plasma treatment. The XRD analysis showed that all TZO films had a (002) preferred orientation, regardless of plasma ambient gas. The FE-SEM and AFM images displayed that the surface grains of the H<sub>2</sub> and Ar + H<sub>2</sub> plasma-treated films were noticeably etched and caused rough surfaces due to etching effect of hydrogen radicals, while the Ar plasma-treated film exhibited the larger grain size than the H<sub>2</sub> and Ar + H<sub>2</sub> plasma-treated ones. The resistivities of all the plasma-treated films decreased and the lowest value was  $1.13 \times 10^{-3} \Omega\text{-cm}$  for the Ar + H<sub>2</sub> plasma-treated sample. The decrements of resistivities for the Ar + H<sub>2</sub>, H<sub>2</sub>, and Ar plasma-treated films were 62%, 51%, and 27%, respectively. After plasma treatment, the average visible transmittance slightly increased over 82% (including glass substrate) and the optical energy band-gap broadened. The Haacke's figure of merit ( $\rho$ ) increased for all the plasma-treated films and the Ar + H<sub>2</sub> plasma treatment made  $\rho$  increase more than the others. Therefore, this work concludes that the Ar + H<sub>2</sub> plasma treatment is more effective than H<sub>2</sub> and Ar plasma treatment in improving opto-electronic properties of the TZO films. The developed Ar + H<sub>2</sub> plasma-treated TZO films are suitable as TCO material for opto-electronic device applications.

#### Acknowledgements

The authors acknowledge Ministry of Science and Technology of Taiwan under the Grant NSC 102-2221-E-005-068 and MOST 103-2221-E-005-040-MY2 for financial support. We also thank Dr. Chia-Cheng Huang for assistance in target fabrication.

## References

- [1] K. Zhang, A.R. Forouhi, I. Bloomer, Accurate and rapid determination of thickness,  $n$  and  $k$  spectra, and resistivity of indium–tin–oxide films, *J. Vac. Sci. Technol. A* 17 (1999) 1843–1847.
- [2] E.H. Ko, H.J. Kim, S.J. Lee, J.H. Lee, H.K. Kim, Nano-sized Ag inserted into ITO films prepared by continuous roll-to-roll sputtering for high-performance, flexible, transparent film heaters, *RSC Adv.* 6 (2016) 46634–46642.
- [3] K.A. John, R.R. Philip, P. Sajan, T. Manju, In situ crystallization of highly conducting and transparent ITO thin films deposited by RF magnetron sputtering, *Vacuum* 132 (2016) 91–94.
- [4] T. Minami, H. Nanto, S. Takata, Highly conductive and transparent aluminum doped zinc oxide thin films prepared by rf magnetron sputtering, *Jpn. J. Appl. Phys.* 23 (1984) L280–L282.
- [5] O. Gürbüza, İ. Kurtb, S. Çalışkanb, S. Güner, Influence of Al concentration and annealing temperature on structural, optical, and electrical properties of Al co-doped ZnO thin films, *Appl. Surf. Sci.* 349 (2015) 549–560.
- [6] H.P. Chang, F.H. Wang, J.C. Lin, C.Y. Kung, H.W. Liu, Enhanced conductivity of aluminum doped ZnO films by hydrogen plasma treatment, *Thin Solid Films* 518 (2010) 7445–7449.
- [7] F.H. Wang, H.P. Chang, C.C. Tseng, C.C. Huang, Effects of H<sub>2</sub> plasma treatment on properties of ZnO: Al thin films prepared by RF magnetron sputtering, *Surf. Coat. Technol.* 205 (2011) 5269–5277.
- [8] F.H. Wang, K.N. Chen, C.M. Hsu, M.C. Liu, C.F. Yang, Investigation of the structural, electrical, and optical properties of the nano-scale GZO thin films on glass and flexible polyimide substrates, *Nanomater* 6 (2016) 88.
- [9] T. Minami, H. Sato, H. Nanto, S. Takata, Group III impurity doped zinc oxide thin films prepared by rf magnetron sputtering, *Jpn. J. Appl. Phys.* 24 (1985) L781–L784.
- [10] L.P. Peng, L. Fang, X.F. Yang, H.B. Ruan, Y.J. Li, Q.L. Huang, C.Y. Kong, Characteristics of ZnO: Al thin films prepared by RF magnetron sputtering, *Phys. E* 41 (2009) 1819–1823.
- [11] S.S. Lin, J.L. Huang, D.F. Lii, Effect of substrate temperature on the properties of Ti-doped ZnO films by simultaneous rf and dc magnetron sputtering, *Mat. Chem. Phys.* 90 (2005) 22–30.
- [12] J.L. Chung, J.C. Chen, C.J. Tseng, The influence of titanium on the properties of zinc oxide films deposited by radio frequency magnetron sputtering, *Appl. Surf. Sci.* 254 (2008) 2615–2620.
- [13] J.L. Chung, J.C. Chen, C.J. Tseng, Preparation of TiO<sub>2</sub>-doped ZnO films by radio frequency magnetron sputtering in ambient hydrogen–argon gas, *Appl. Surf. Sci.* 255 (2008) 2494–2499.
- [14] Y.R. Park, K.J. Kim, Optical and electrical properties of Ti-doped ZnO films: observation of semiconductor–metal transition, *Solid State Commun.* 123 (2002) 147–150.
- [15] J.J. Lu, Y.M. Lu, S.I. Tasi, T.L. Hsiung, H.P. Wang, L.Y. Jang, Conductivity enhancement and semiconductor–metal transition in Ti-doped ZnO films, *Opt. Mater* 29 (2007) 1548–1552.
- [16] F.H. Wang, Jen-Chi Chao, Han-Wen Liu, Tsung-Kuei Kang, Physical properties of ZnO thin films codoped with titanium and hydrogen prepared by RF magnetron sputtering with different substrate temperatures, *J. Nanomater* 2015 (2015) 936482.
- [17] G. Fang, D. Li, B.L. Yao, Fabrication and vacuum annealing of transparent conductive AZO thin films prepared by DC magnetron sputtering, *Vacuum* 68 (2003) 363–372.
- [18] B.Y. Oh, M.C. Jeong, D.S. Kim, W. Lee, J.M. Myoung, Post-annealing of Al-doped ZnO films in hydrogen atmosphere, *J. Cryst. Growth* 281 (2005) 475–480.
- [19] J. Wang, Y. Mei, X. Lu, X. Fan, D. Kang, P. Xu, T. Tan, Effects of annealing pressure and Ar<sup>+</sup> sputtering cleaning on Al-doped ZnO films, *Appl. Surf. Sci.* 387 (2016) 779–783.
- [20] Y. Yamada, K. Kadowaki, H. Kikuchi, S. Funaki, S. Kubo, Positional variation and annealing effect in magnetron sputtered Ga-doped ZnO films, *Thin Solid Films* 609 (2016) 25–29.
- [21] S. Major, S. Kumar, M. Bhatnagar, K.L. Chopra, Effect of hydrogen plasma treatment on transparent conducting oxides, *Appl. Phys. Lett.* 49 (1986) 394–396.
- [22] S.J. Baik, J.H. Jang, C.H. Lee, W.Y. Cho, K.S. Lim, Highly textured and conductive undoped ZnO film using hydrogen post-treatment, *Appl. Phys. Lett.* 70 (1997) 3516–3518.
- [23] N. Ohashi, Y.G. Wang, T. Ishigaki, Y. Wada, H. Taguchi, I. Sakaguchi, T. Ohgaki, Y. Adachi, H. Haneda, Lowered stimulated emission threshold of zinc oxide by hydrogen doping with pulsed argon–hydrogen plasma, *J. Cryst. Growth* 306 (2007) 316–320.
- [24] F.H. Wang, H.P. Chang, J.C. Chao, Improved properties of Ti-doped ZnO thin films by hydrogen plasma treatment, *Thin Solid Films* 519 (2011) 5178–5182.
- [25] P.F. Cai, J.B. You, X.W. Zhang, J.J. Dong, X.L. Yang, Z.G. Yin, N.F. Chen, Enhancement of conductivity and transmittance of ZnO films by post hydrogen plasma treatment, *J. Appl. Phys.* 105 (2009) 083713.
- [26] Y.M. Strzemechny, H.L. Mosbacher, D.C. Look, D.C. Reynolds, C.W. Litton, N.Y. Garces, N.C. Giles, L.E. Halliburton, S. Niki, L.J. Brillson, Remote hydrogen plasma doping of single crystal ZnO, *Appl. Phys. Lett.* 84 (2004) 2545–2547.
- [27] W.F. Liu, G.T. Du, Y.F. Sun, J.M. Bian, Y. Cheng, T.P. Yang, Y.C. Chang, Y.B. Xu, Effects of hydrogen flux on the properties of Al-doped ZnO films sputtered in Ar+ H<sub>2</sub> ambient at low temperature, *Appl. Surf. Sci.* 253 (2007) 2999–3003.
- [28] C.G. Van de Walle, Hydrogen as a cause of doping in zinc oxide, *Phys. Rev. Lett.* 85 (2000) 1012–1015.
- [29] G. Sanon, R. Rup, A. Mansingh, Growth and characterization of tin oxide films prepared by chemical vapour deposition, *Thin Solid Films* 190 (1990) 287–301.
- [30] R. Das, S. Ray, Zinc oxide—a transparent, conducting IR-reflector prepared by rf-magnetron sputtering, *J. Phys. D: Appl. Phys.* 36 (2003) 152–155.
- [31] R. Banerjee, S. Ray, N. Basu, A.K. Batabyal, A.K. Barua, Degradation of tin-doped indium-oxide film in hydrogen and argon plasma, *J. Appl. Phys.* 62 (1987) 912–916.
- [32] R. Das, T. Jana, S. Ray, Degradation studies of transparent conducting oxide: a substrate for microcrystalline silicon thin film solar cells, *Sol. Energy Mat. Sol. Cells* 86 (2005) 207–216.
- [33] C.S. Prajapati, P.P. Sahay, Effect of precursors on structure, optical and electrical properties of chemically deposited nanocrystalline ZnO thin films, *Appl. Surf. Sci.* 258 (2012) 2823–2828.
- [34] S.T. Tan, B.J. Chen, X.W. Sun, W.J. Fan, H.S. Kwok, Blueshift of optical band gap in ZnO thin films grown by metal-organic chemical-vapor deposition, *J. Appl. Phys.* 98 (2005) 013505.
- [35] E. Burstein, Anomalous optical absorption limit in InSb, *Phys. Rev.* 93 (1954) 632–633.
- [36] B.E. Selnelius, K.F. Berggren, Z.C. Jin, I. Hamberg, C.G. Granqvist, Band-gap tailoring of ZnO by means of heavy Al doping, *Phys. Rev. B* 37 (1988) 10244–10248.
- [37] M. Chen, Z.L. Pei, X. Wang, C. Sun, L.S. Wen, Structural, electrical, and optical properties of transparent conductive oxide ZnO: Al films prepared by dc magnetron reactive sputtering, *J. Vac. Sci. Technol. A* 19 (2001) 963–970.
- [38] K.H. Kim, K.C. Park, D.Y. Ma, Structural, electrical and optical properties of aluminum doped zinc oxide films prepared by radio frequency magnetron sputtering, *J. Appl. Phys.* 81 (1997) 7764.
- [39] G. Haacke, New figure of merit for transparent conductors, *J. Appl. Phys.* 47 (1976) 4086–4089.